Atmospheric deposition of microplastics in Shiraz, Iran

Abbasi, S

10.1016/j.apr.2023.101977
Atmospheric Pollution Research
Elsevier BV

Atmospheric deposition of microplastics in Shiraz, Iran

Sajjad Abbasi [1,2, *], Farnaz Ahmadi [3], Nafiseh Khodabakhshloo [2], Haniye Pourmahmood [2], Atefeh Esfandiari [4], Zeinab Mokhtarzadeh [1], Shaqayeq Rahnama [2], Reza Dehbandi [5], Arya Vazirzadeh [6], Andrew Turner [7]

1. Department of Earth Sciences, School of Science, Shiraz University, Shiraz, 71454, Iran

2. Centre for Environmental Studies and Emerging Pollutants (ZISTANO), Shiraz University, Shiraz, Iran

3. Soil Science Department, Faculty of Agricultural Engineering and Technology, University of Tehran, Vardavard, Karaj 41889-58643, Iran

4. Department of Chemical Engineering, School of Chemical and Petroleum Engineering, Shiraz University, Shiraz, 71454, Iran

5. Environmental Technologies Research Center, Ahvaz Jundishapur University of Medical Sciences, Ahvaz, Iran

6. Department of Natural Resources and Environmental Engineering, School of Agriculture, Shiraz University, Shiraz 71441-65186, Iran

7. School of Geography, Earth and Environmental Sciences, Plymouth University, PL4 8AA, UK

Corresponding author.

Sajjad Abbasi, Email address: sajjad.abbasi@shirazu.ac.ir; sajjad.abbasi.h@gmail.com

Scopus Author ID: https://www.scopus.com/authid/detail.uri?authorId=57203061256

Google scholar: https://scholar.google.com/citations?user=cQzmYz8AAAAJ&hl=en&oi=ao

ORCID: 0000-0002-5194-9334

Accepted 25th October 2023

https://doi.org/10.1016/j.apr.2023.101977

Highlights

Atmospheric microplastics (MPs) accumulate during dry weather over Shiraz

Subsequently, MPs rapidly wash out with incipient rain

Deposition decreases and is lowest when rainfall ceases and the cycle continues

MPs dominated by fibres but no clear relationship between deposition mode and fibre size

Variability of MP deposition in the literature may reflect environmental conditions

Abstract

The atmosphere plays a critical role in the regional and global transportation and redistribution of microplastics (MPs). However, the significance of rainfall and its means of scavenging MPs are not well understood. In this study, MP deposition was determined during successive dry and rainy events over eight consecutive days in the Shiraz region of Iran. Flux magnitudes and temporal distributions at six sites within and outside the city (including a remote, non-urbanised location) were similar and revealed a progressive increase in MP abundance and deposition during dry periods (up to about 50 MP m^{-2} h^{-1}) and subsequent relatively rapid wet deposition (washout) by incipient rainfall (peaking at about 130 MP m^{-2} h^{-1}). Wet deposition of MPs progressively decreased throughout the rainfall event, but with evidence of secondary peaks, before atmospheric accumulation and dry deposition increased during the next dry event and the cycle continued. Dry and wet deposition were dominated by fibres (that included polyester-polyethylene terephthalate, polystyrene, polyvinyl chloride and polyethylene) but the evolution of deposition did not appear to be associated with changes in MP size. These observations indicate that, as with other airborne pollutants, initial rainfall is an efficient scavenger of atmospheric MPs. Along with variations in methodology, this effect may contribute to the wide variation in MP fluxes reported in the literature.

Keywords: fibres; accumulation; precipitation; airborne; scavenging

1. Introduction

It is becoming increasingly evident that the atmosphere is a key temporary reservoir for microplastics (MPs; < 5 mm in size) (Dris et al., 2016; Wright et al., 2020; Zhang et al., 2020;). As a consequence, MPs, and in particular those of a fibrous nature, may be transported long distances from their direct sources and have been detected in regions remote from centres of urbanisation and industrialisation (Allen et al., 2019; Brahney et al., 2020; Ding et al., 2021; Villanova-Solano et al., 2023).

The significance of airborne MPs is often quantified in terms of dry, wet or bulk deposition; that is, near-ground level deposition rate over a specific area and usually expressed as number per m^2 per day. On this basis, independent results have revealed variations spanning many orders of magnitude (Purwiyanto et al., 2022; Li et al., 2023). Part of this variation may be attributed to differences in sampling, processing and analytical detection limits and distances from known sources, but environmental factors are also important. In particular, rainfall is believed to wash out MPs from the atmosphere by wet deposition, and it has been suggested that the efficacy of this effect may be related to rainfall intensity and duration and rain droplet size (Szewc et al., 2021; Yuan et al., 2023). However, the precise means and timeframes involved in MP scavenging by rainfall are not well understood, largely because most studies have considered aggregated deposition or net accumulation over extended periods or entire events (Abbasi and Turner, 2021; Huang et al., 2021; Li et al., 2023).

In a short-term study of a monsoon event, Abbasi (2021) showed that the wet depositional flux of MPs decreased rapidly in the first 30 minutes, providing evidence for the rapid washing out or airborne MPs during seasonal, heavy rainfall. In the present study, the more general role of rainfall in scavenging MPs from the atmosphere was investigated over a longer timeframe that encompasses successive dry and wet events with the hypothesis that wet deposition is not consistent throughout an event. Specifically, dry and wet (or bulk) MP deposition were determined over 24 periods of three to twelve hours each and at six different locations in the region of Shiraz, Iran. MPs were also classified by size and shape in order to evaluate whether these characteristics are impacted by environmental conditions (rainfall, wind speed, humidity) and a selection was analysed for their polymer composition in order to identify the principal plastic types.

2. Material and Methods

2.1. Sample location

Shiraz, southwest Iran, is the fifth most populous city in Iran (about 1.6 million in 2016) and lies on a green plain at about 1600 m above sea level. The city supports an oil refinery and various industries in the electronics, manufacturing and agriculture sectors. The climate is moderate semi-arid with an annual average rainfall, humidity and temperature of 335 mm, 64% and 18 ^{o}C, respectively, and the prevailing wind direction is from the northwest. Samples were collected from the urban metropolis of Shiraz (S1 to S5) and from a station remote from any significant urbanisation (C) located about 40 km to the north and upwind of the city (Figure 1). Regarding the Shiraz sample locations, S1 is a low traffic area on the outskirts of the city and close to agricultural land to the west, S2 and S3 are residential areas of low traffic and a high density of green space, S4 is the northern entrance to the city centre and is adjacent to a major highway, and S5 is a residential area with a moderate amount of traffic.

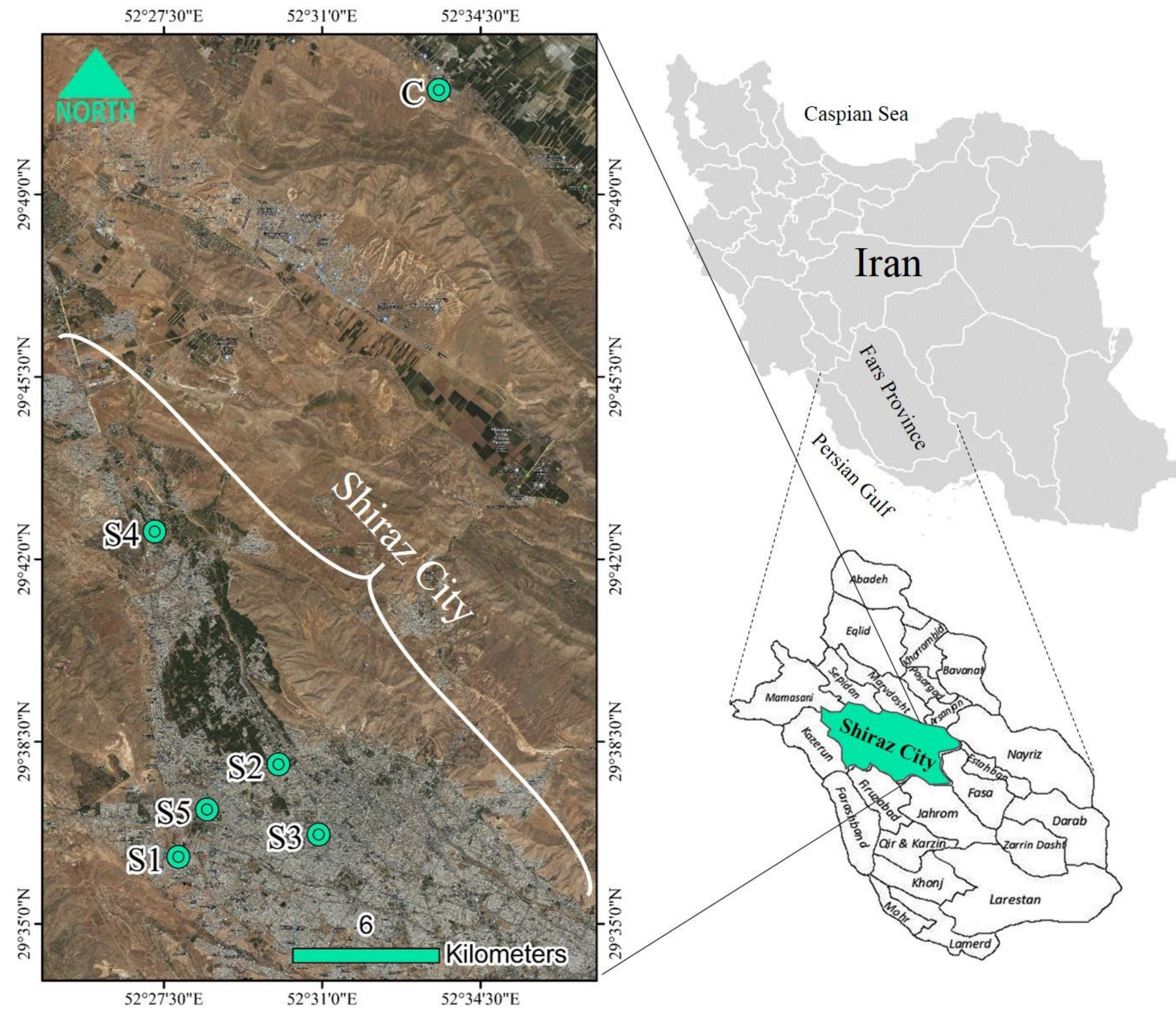

Figure 1: Location of the sampling sites in the Shiraz region. Note the relative remoteness of station C from centres of population (in grey).

2.2. Sampling

After carefully checking the rainfall forecasts, eight consecutive days (192 h) were selected for sampling from 28 December 2021 to 5 Jan 2022. This timescale comprised three dry events (totalling 117 h) and two distinct rainfall regimes (totalling 75 h). Dry events were sampled across 11 periods (labelled D) of twelve hours (plus any remaining time before incipient rain), and rain events were sampled across 13 periods (labelled R) of three to eight hours depending on the duration of precipitation.

Samples were collected at each location in a stainless steel dish (whose depth was 30 cm and aperture diameter ranged from 25 to 43 cm, depending on any constraints imposed by the precise sampling location and position). Each dish was positioned, via a metallic frame, about 2 m above the flat roof of a three-storey building that was exposed in all directions, and at a total elevation of about 10 m above ground level. During dry events, dishes were partly filled with 1-L of 2 μm-filtered, distilled water to aid retention and minimise blowby of dry deposited material. At each site, material collected over the sampling period, plus filtered (< 2 μm), distilled water-rinsings of the dish, were transferred to a 2-L glass bottle with the aid of a glass funnel. During rain events, pre-cleaned (with distilled water) dry dishes were continuously used to collect wet deposited material over each period (although, strictly, bulk deposition was captured). The contents were carefully poured into a graduated glass measuring cylinder to determine rainfall volume. With a Eutech Instruments PCD650 probe, electrical conductivity (as specific conductance and a measure of rainwater chemistry) was then determined before the contents were transferred, with the dish rinsings, to a glass bottle as above.

2.3. Sample processing and microplastic counting and characterisation

The contents of each glass sample bottle were vacuum filtered through a 2 μm pore size S&S filter paper (Blue Band, grade 589/3). Filters were transferred to individual, 60 mL foil-wrapped glass beakers and digested in 35 mL of 30% H_2O_2 (Arman Sina, Tehran) until bubble formation ceased. The contents of the digestions were refiltered through clean 2 μm filters that were subsequently air-dried at 25 ^{o}C for 48 h in a metal cabinet housed in a clean room before being stored in glass Petri dishes.

MPs on each filter were visually identified, counted and characterised (by size, shape and colour) under a stereo digital microscope (Sairan DSM3000) at up to 200 X magnification with the aid of a 250 μm-diameter stainless steel probe and ImageJ software. Identification of MPs was based on shape, colour, size, thickness, shininess, hardness and surface structure according to protocols outlined elsewhere (Abbasi et al., 2019). Classification was based on shape (fibre, film, fragment or spherule) and length of the longest axis, L (L < 100 μm, 100 ≤ L < 250 μm, 250 ≤ L < 500 μm, 500 ≤ L < 1000 μm, L > 1000 μm; and with a size detection limit estimated to be between 30 and 50 μm depending on shape). The polymeric composition of 34 MPs (or about 4% of the total) of a range of shapes, sizes and colours and collected from different locations and meteorological conditions was determined using a micro-Raman spectrometer (μ-Raman-532-Ci, Avantes, Apeldoorn, Netherland) with a laser of 785 nm and Raman shift of 400-1800 cm^{-1}.

2.4. Laboratory cleanliness and quality assurance

Laboratory equipment was washed with phosphate-free soap, double-rinsed with distilled water and soaked in 10% HNO_3 for 24 h before being rinsed twice with filtered, distilled water, dried at room temperature in a customised clean room and protected by Al foil. Laboratory work surfaces were cleaned with ethanol, laboratory clothing was cotton-based and all reagents and solutions were filtered through 2 μm before being used. Under these conditions, processing of distilled water contained in glass bottles as above revealed no MP contamination. The number of MPs on ten random (sample) filters were recounted under the microscope and returned the same values as the original counts.

3. Results

Table 1 shows the duration of each sampling event, along with an indication of regional wind speed, wind direction and relative humidity (obtained from ventusky.com) for each period. Average wind speeds ranged from < 5 to 10 - 15 km h^{-1} and usually had a southerly and/or westerly component. Relative humidity exceeded 80% during the rain events but was more variable during dry events (between 10% and 90%). Also shown for each rainy period is rainfall (in mm), derived from the volume of precipitation collected and the area of the metal collecting dish, along with the measured specific electrical conductance of rainwater. For a given period, rainfall exhibited some variation among the different locations, and in particular the highest values were frequently reported for S4 to the north of the city. Overall, average rainfall intensity (i.e., mean periodic rainfall for all locations normalised to sampling duration) ranged from about 0.25 mm h^{-1} for R6 to > 2.2 mm h^{-1} for R18, and specific electrical conductance, as a measure of rainwater chemistry, ranged from about 20 to 270 μs cm^{-1}, with the highest values at each location usually encountered towards the beginning of both rain events.

Table 2 presents the number of MPs retrieved from the filters at each location and for each sampling period, along with the number normalised per m^2 of sampling area and per h of collection time (i.e., deposition rate). In total, 132 samples were collected and analysed (twelve were unsuccessfully retrieved or lost), and in all but eleven of these samples MPs were identified.

The number of MPs in each sample was > 20 in eleven cases, and the maximum number of MPs was 47. When normalised, deposition rates (where detected) ranged from < 1 m^{-2} h^{-1} (< 24 m^{-2} d^{-1}) in three samples taken during dry conditions to > 100 m^{-2} h^{-1} (> 2400 m^{-2} d^{-1}) in three samples collected during rain events.

Table 1: Duration of the dry (D) and rainy (R) sampling events and periods, along with indicative, average (by rank) regional wind speeds and directions and relative humidities. Periodic rainfall, derived from the volume of precipitation and area of sample capture, and specific electrical conductance (EC) of rainwater, are shown for each location. Note that NC denotes no sample collection and LS denotes a lost sample.

							C	S1	S2	S3	S4	S5
sampling period	event	duration, h	time since start, h	wind speed, km h^{-1}	wind direction	humidity, %	rainfall, mm (EC, µS cm^{-1})					
D1		12	12	< 5	SW, SE	10-30						
D2	1	12	24	10-15	SW, W	10-30						
D3		3	27	< 5	S	30						
R4		3	30	< 5	SW	90	0.93 (140)	3.06 (50)	2.21 (150)	1.48 (140)	1.86 (200)	LS
R5		5	35	10-15	SW, S	90	1.36 (80)	4.39 (70)	2.65 (80)	2.55 (90)	5.00 (130)	3.49 (50)
R6		5	40	< 5	SW	90	NC	1.12 (90)	2.82 (20)	0.55 (190)	0.99 (270)	0.63 (130)
R7	2	8	48	< 5	S	90	1.12 (70)	5.10 (30)	2.92 (80)	3.55 (80)	4.65 (90)	0.93 (50)
R8		6	54	< 5	SE	90	2.44 (50)	6.53 (20)	4.91 (30)	6.14 (50)	4.94 (50)	6.40 (30)
R9		5	59	< 5	S	90	9.88 (30)	6.51 (20)	5.18 (20)	4.29 (40)	12.50 (90)	10.23 (40)
R10		5	64	5-10	SW	90	1.80 (150)	3.06 (20)	3.94 (20)	4.29 (70)	4.10 (90)	1.10 (110)
R11		8	72	< 5	W	90	NC	9.84 (20)	6.28 (20)	9.82 (20)	15.56 (170)	8.84 (50)
D12		12	84	< 5	SW	40-90						
D13	3	12	96	< 5	SW	70						
D14		12	108	10-15	SW, S	40-70						
D15		6	114	< 5	SW	70						
R16		6	120	< 5	SE	80-90	1.05 (140)	3.67 (40)	1.42 (60)	2.62 (100)	2.79 (170)	7.05 (30)
R17		6	126	10-15	SE, S	90-100	8.72 (20)	12.76 (20)	7.08 (60)	12.44 (40)	10.16 (70)	9.53 (30)
R18	4	5	131	< 5	S	100	NC	LS	9.69 (20)	7.24 (40)	20.70 (40)	6.40 (50)
R19		5	136	< 5	S	90-100	5.12 (20)	LS	2.43 (30)	3.21 (80)	7.91 (70)	2.73 (30)
R20		8	144	< 5	S, W	80-90	7.38 (50)	LS	6.33 (30)	5.06 (70)	11.63 (70)	7.56 (50)
D21		12	156	5-10	SW	50-70						
D22	5	12	168	5-10	SW, S	80						
D23		12	180	10-15	NW, W	40-80						
D24		12	192	< 5	SW	60						

Table 2: The number of MPs and the number of MPs per m^2 per h for each sampling event and sampling period and for each location. Note that NC denotes no sample collection and LS denotes a lost sample.

		no. MPs						MP m^{-2} h^{-1}					
sampling period	event	C	S1	S2	S3	S4	S5	C	S1	S2	S3	S4	S5
D1		6	4	13	9	12	4	5.8	6.8	9.6	5.2	11.6	3.9
D2	1	9	11	18	21	20	15	8.7	18.7	13.3	12.1	19.4	14.5
D3		6	3	15	7	12	3	23.3	20.4	44.2	16.1	46.5	11.6
R4		4	19	20	12	26	LS	15.5	129.3	59.0	27.6	100.8	LS
R5		44	10	11	12	25	20	102.3	40.8	19.5	16.6	58.1	46.5
R6		NC	6	3	2	1	12	NC	24.5	5.3	2.8	2.3	27.9
R7	2	13	5	1	4	8	2	18.9	12.8	1.1	3.4	11.6	2.9
R8		17	6	2	5	2	3	32.9	20.4	2.9	5.7	3.9	5.8
R9		4	4	2	4	0	1	9.3	16.3	3.5	5.5	0	2.3
R10		2	6	2	10	18	3	4.7	24.5	3.5	13.8	41.9	7.0
R11		NC	1	1	2	14	3	NC	2.6	1.1	1.7	20.3	4.4
D12		0	0	1	1	4	1	0	0	0.7	0.6	3.9	1.0
D13	3	1	0	2	5	LS	6	1.0	0	1.5	2.9	LS	5.8
D14		0	1	4	8	4	7	0	1.7	2.9	4.6	3.9	6.8
D15		4	2	0	0	2	10	7.8	6.8	0	0	3.9	19.4
R16		5	5	8	5	13	14	9.7	17.0	11.8	5.7	25.2	27.1
R17		14	3	9	20	18	1	27.1	10.2	13.3	23.0	34.9	1.9
R18	4	NC	LS	2	47	3	3	NC	LS	3.5	64.8	7.0	7.0
R19		1	LS	8	2	2	1	2.3	LS	14.2	2.8	4.7	2.3
R20		2	LS	11	5	1	1	2.9	LS	12.2	4.3	1.5	1.5
D21		1	1	4	1	1	0	1.0	1.7	2.9	0.6	1.0	0
D22	5	4	LS	0	8	4	0	3.9	LS	0	4.6	3.9	0
D23		2	LS	9	20	LS	7	1.9	LS	6.6	11.5	LS	6.8
D24		5	LS	10	21	5	0	4.8	LS	7.4	12.1	4.8	0

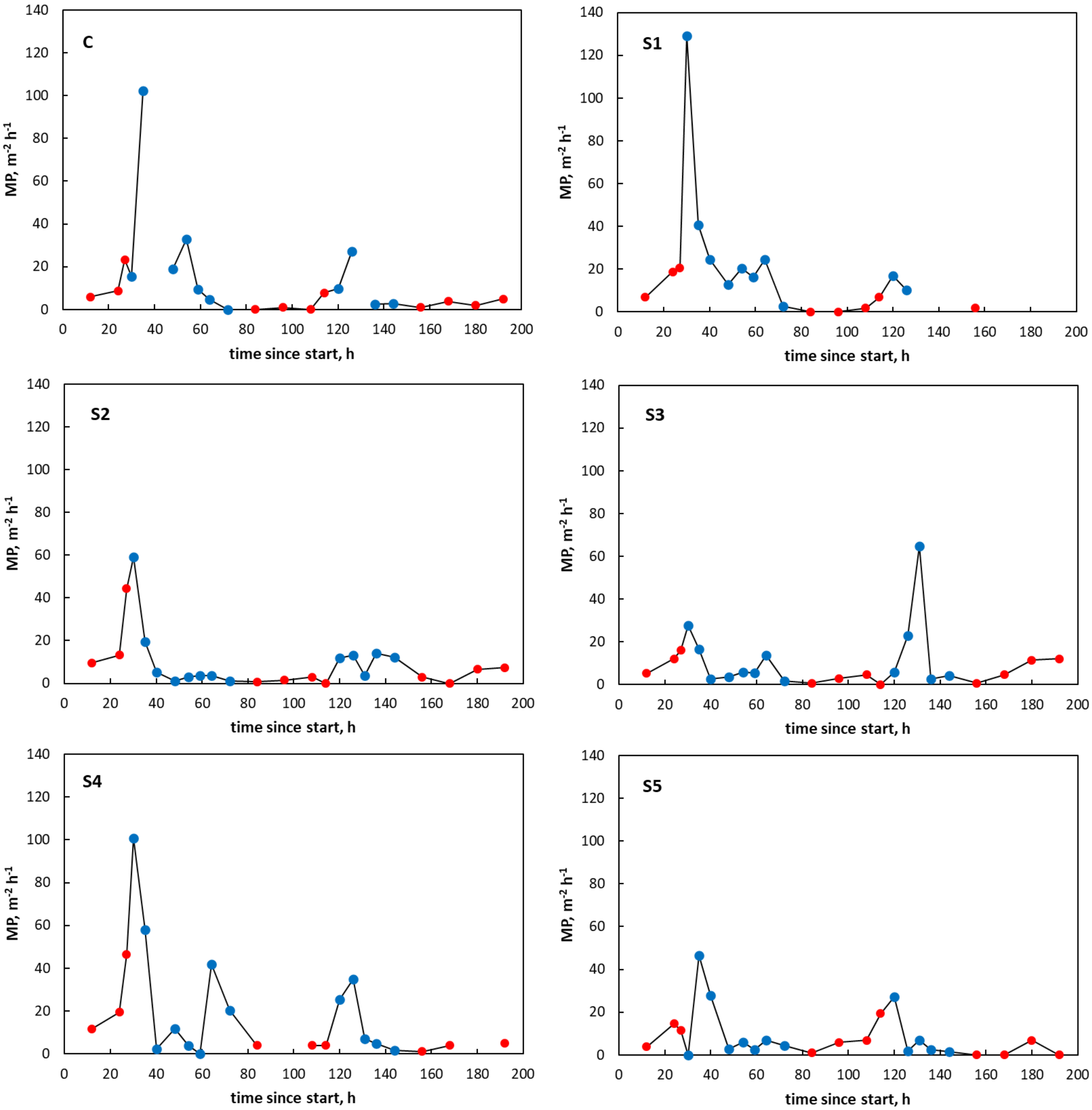

Figure 2: MP deposition as a function of time at the six locations (C and S1 to S5). Dry events are shown in red and rain events are shown in blue. Note the discontinuities where samples were lost or not collected (see caption to Figure 2).

The evolution of MP deposition over the entire timeframe studied is illustrated for all six locations in Figure 2. Distributions were broadly similar at each location and consisted of an initial dry event in which deposition increased, followed by a rain event in which deposition rapidly peaked and subsequently declined but with evidence of a secondary peak whose precise timing was more variable. Low MP deposition was observed in the subsequent dry event, which exhibited an increase at three locations, before the second precipitation event in which deposition exhibited a persistent peak of variable magnitude and timing. During the final dry event, deposition was again low, and in most cases exhibited an increase as a function of time.

With the exception of seven fragments (sampled in both dry and rainy conditions), all MPs detected in the study were fibres of varying lengths, thicknesses and colours. The size distributions of MPs, combined for all locations, are shown in Figure 3 by sampling event (defined in Table 1). For all dry and rain events, the largest (> 1000 μm) and smallest (< 100 μm) size categories were most important, with a combined proportion that averages about two-thirds, and remaining MPs were distributed among the three intermediate size classifications.

The results of the Raman analysis are summarised in Figure 4. Here, 31 fibres and three fragments were analysed from various locations and events. Polyethylene terephthalate-polyester was the dominant polymer (> 50%), with additional contributions from polyvinyl chloride, polytetrafluoroethylene, polystyrene, polypropylene, polyethylene and nylon.

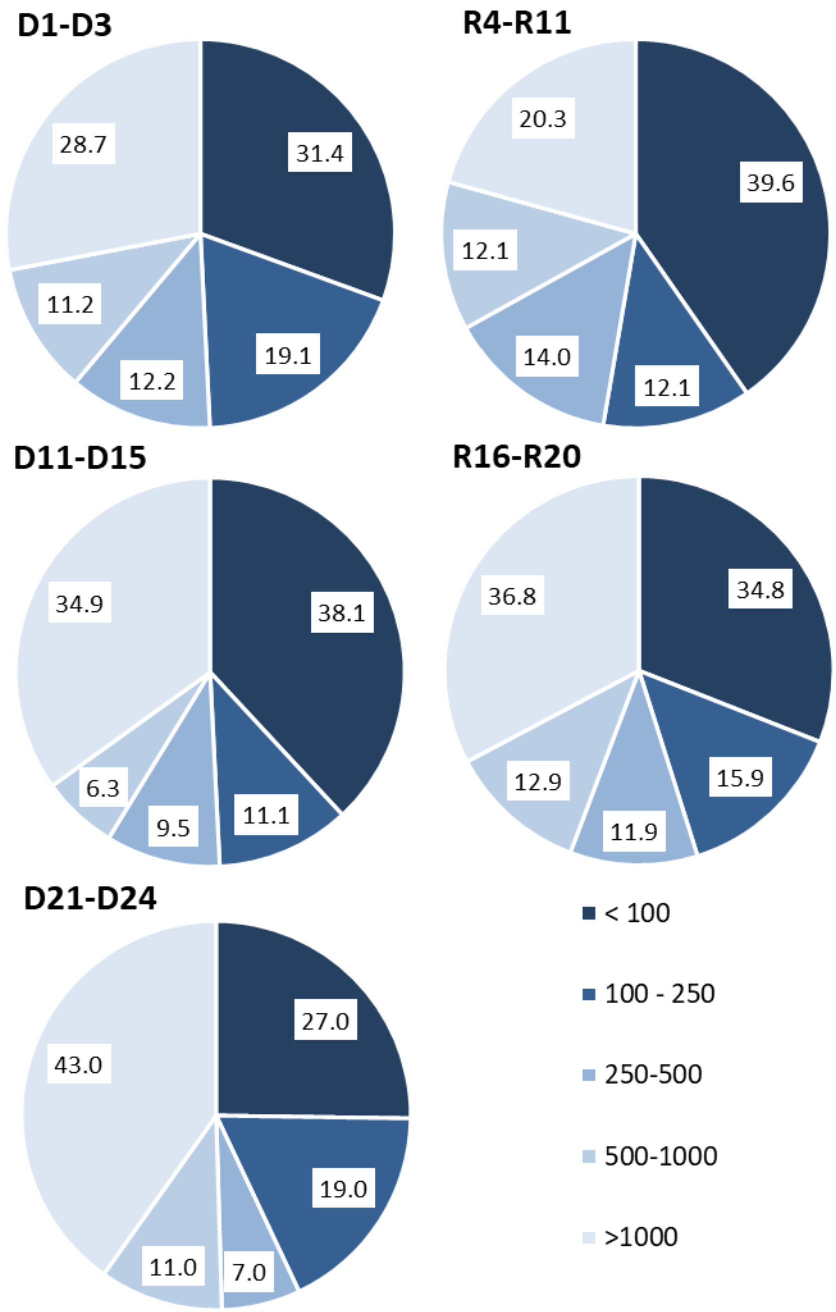
D1-D3
31.4
19.1
12.2
11.2
28.7
R4-R11
39.6
12.1
14.0
12.1
20.3
D11-D15
38.1
11.1
9.5
6.3
34.9
R16-R20
34.8
15.9
11.9
12.9
36.8
D21-D24
27.0
19.0
7.0
11.0
43.0
< 100
100 - 250
250-500
500-1000
>1000

Figure 3: Percentage distribution of MPs by size (L, in μm) for five different dry (D) and rain (R) events (see Table 1).

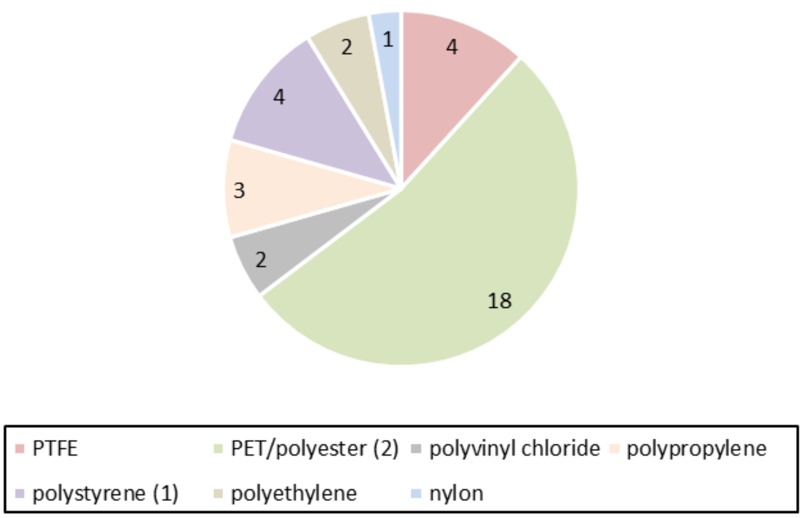

Figure 4: Distribution of MPs by polymer type (n = 34). PET = polyethylene terephthalate, PTFE = polytetrafluoroethylene, and numbers in parentheses in the legend denote non-fibrous samples (fragments).

4. Discussion

Based on our sampling design and identification protocols, the broad, qualitative findings of the present study are in agreement with those from other studies examining the presence or deposition of atmospheric MPs in urban and more remote areas, and either in dry conditions or during rainfall or both. Here, fibres of varying lengths are the most abundant shape of MP, presumably because of their favourable aerodynamic properties, and PET-polyester is the most common (or one of most common) petroleum-based polymer/s (Wright et al., 2020; Abbasi and Turner, 2021; Ding et al., 2021; Huang et al., 2021; Purwiyanto et al., 2021; Jia et al., 2022; Liu et al., 2022; Perera et al., 2022; Chang et al., 2023; Li et al., 2023). The dominance of polyester-based fibres suggest that clothing and textiles are the most important primary source of airborne MPs, with secondary distal sources likely to include resuspension from soils and agricultural land applied with contaminated sewage sludge (Brahney et al., 2020; Rezaei et al., 2022).

Atmospheric deposition rates of MPs reported in the literature vary widely. For example, Purwiyanto et al. (2022) determined fluxes between 3 and 40 MPs m^{-2} d^{-1} in coastal Jakarta, while Jia et al. (2022) report an average of 3261 MPs m^{-2} d^{-1} in Shanghai during the rainy season and Li et al. (2023) report a maximum of 75,000 MPs m^{-2} d^{-1} in a rural region of northern China. Geographical and temporal variations have been attributed to seasonal and climatic conditions (Huang et al., 2021; Hernández-Fernández et al., 2022) and proximity to urban areas (Shruti et al., 2022; Sun et al., 2022), as well as differences in sample collection (including height above ground level) and processing and means of plastic identification (Knobloch et al., 2021; Szewc et al., 2021). For example, we note that Li et al. (2023) sampled at only 100 cm above ground level and report rayon as the dominant polymer type, indicating that semi-synthetic fibres were considered alongside petroleum-based polymers.

One of the key factors determining the nature and magnitude of atmospheric MP depositional flux is the mode of deposition (dry deposition versus wet deposition). Dry deposition is determined by deposition velocity (particle size and shape) and is also specific to meteorological conditions and landcover type (Klein et al., 2019; Szewc et al., 2021), while rainfall acts to scavenge MPs from the atmosphere (Zhang et al., 2020). Many studies have found that, for a given sampling time, wet deposition is greater than dry deposition, or at least bulk deposition is greater during wet periods than dry periods (Dris et al., 2016; Huang et al., 2021; Liu et al., 2022; Li et al., 2023; Yuan et al., 2023). However, these studies have only considered daily or cumulative rainfall and have acknowledged that other factors, like rainfall height, intensity and frequency and droplet size, could be important. The potential effects of rainfall intensity and duration on MP deposition were demonstrated by Abbasi (2021) during the onset of a monsoon event in Shiraz. Here, MP deposition rate rapidly declined during the first 30 minutes of heavy precipitation.

The present study has determined MP deposition with a relatively high temporal resolution (several hours, and with MPs reported per m^{-2} per h) over consecutive dry and rain events and, therefore, affords a greater insight into the role that rainfall plays in MP transport. Thus, across six locations within the vicinity of Shiraz that includes a more remote location, and despite different land uses and local sources of MPs, distributions and magnitudes of deposition across the entire sampling timeframe are similar.

Specifically, an initial dry weather event, with southerly winds and low humidity, allows MPs from local and distal sources to progressively build up in the atmosphere and deposit through gravitational settlement. Incipient rainfall acts to rain out and wash out these MPs (through in-cloud and below-cloud scavenging, respectively; Audoux et al., 2023), resulting in a spike in wet deposition with little or no lag. Subsequent precipitation encounters “cleaner” air and depositional fluxes decline to a low, residual value. A secondary peak in deposition could be related to a spell of relatively high rainfall (and, presumably, relatively large raindrops that increase collision frequencies; Guo et al., 2016) coupled with winds with an easterly component (Table 1) that introduce MPs from a different region. Specific electrical conductance follows these broad trends, reflecting the propensity of rainfall to concurrently washout airborne salts from the atmosphere.

The ensuing dry event is accompanied by an immediate period of low deposition (initially, no MPs were detected at C and S1), and although there is often a subsequent build-up of MPs, the increase is not as marked as that observed during the initial dry event. Presumably, this reflects the effects of preceding rainfall in cleansing atmospheric MPs and the wetting of regional soils that inhibits MP resuspension (Abbasi and Turner, 2021). An additional contributing factor could be that rainfall here began in the early hours of the next day when local MP-generating activities were minimal. The next rainfall event is accompanied by a smaller peak that reflects the washing out of lower numbers of locally resuspended and regionally advected MPs, with the final dry event beginning with very little MP deposition and exhibiting evidence that the preceding cycle is repeated.

The intra- and inter-event patterns that we observed for MPs, and in particular those during incipient rainfall, have been documented for other aerosols more generally (Battarbee et al., 1997; Castro et al., 2010; Fujino and Miyamoto, 2022). Here, washout is usually reported to be greater for larger particles, and although this effect was not evident from our results, it must be borne in mind that the more general literature deals with much smaller and higher density particulate matter. Consistent with other independent studies, rainfall acts to remove MPs from the atmosphere, at least temporarily.

In summary, average MP depositional fluxes were similar among multiple locations with different characteristics within the Shiraz region, and significant (at least order of magnitude) intra-location variations observed during different meteorological conditions. These findings support previous assertions that MPs are ubiquitous contaminants, but also suggest that variations reported in the literature may result, to a significant extent, from environmental conditions and not, necessarily, proximity to source regions. Specifically, it would appear that incipient rainfall is a critical driver for the scavenging of MPs from the atmosphere through below-cloud washout. It is surmised that rainfall also acts to inhibit MP resuspension from certain surfaces (e.g., soils) through ground dampening.

Acknowledgements

We acknowledge financial support from Shiraz University (grant number: 0GRC1M371631) and technical support from staff at the Centre for Environmental Studies and Emerging Pollutants (ZISTANO).

References

Abbasi, S., 2021. Microplastics washout from the atmosphere during a monsoon rain event. Journal of Hazardous Materials Advances 4, 100035.

Abbasi, S., Turner, A., 2021. Dry and wet deposition of microplastics in a semi-arid region (Shiraz, Iran). Science of the Total Environment 786, 147358.

Allen, S., Allen, D., Phoenix, V.R., Roux, G.L., Jim´enez, P.D., Simonneau, A., Binet, S., Galop, D., 2019. Atmospheric transport and deposition of microplastics in a remote mountain catchment. Nature Geosciences 12, 339–344.

Audoux, T., Laurent, B., Chevallier, S., Feron, A., Pangui, E., Maisonneuve, F., Desboeufs, K., Triquet, S., Noyalet, G., Lauret, O., Huet, F., 2023. Automatic sequential rain sampling to study atmospheric particulate and dissolved wet deposition. Atmospheric Environment 295, 119561.

Battarbee, J.L., Rosel, N.L., Long, X., 1997. A continuous, high resolution record of urban airborne particulates suitable for retrospective microscopical analysis. Atmospheric Environment 31, 171-181.

Brahney, J., Hallerud, M., Heim, E., Hahnenberger, M., Sukumaran, S., 2020. Plastic rain in protected areas of the United States. Science 368, 1257–1260.

Castro, A., Alonso-Blanco, E., González-Colino, M., Calvo, A.I., Fernández-Raga, M., Fraile, R., 2010. Aerosol size distribution in precipitation events in León, Spain Atmospheric Research 96, 421-435.

Chang, D.Y., Jeong, S., Shin, J., Park, J., Park, C.R., Choi, S., Chun, C.H., Chae, M.Y., Lim, B.C., 2023. First quantification and chemical characterization of atmospheric microplastics observed in Seoul, South Korea. Environmental Pollution 327, 121481.

Ding, Y., Zou, X., Wang, C., Feng, Z., Wang, Y., Fan, Q., Chen, H., 2021. The abundance and characteristics of atmospheric microplastic deposition in the northwestern South China Sea in the fall. Atmospheric Environment 253, 118389.

Dris, R., Gasperi, J., Saad, M., Mirande, C., Tassin, B., 2016. Synthetic fibers in atmospheric fallout: a source of microplastics in the environment? Marine Pollution Bulletin 104, 290–293.

Fujino, R., Miyamoto, Y., 2022. $PM_{2.5}$ decrease with precipitation as revealed by single-point ground-based observation. Atmospheric Science Letters 23, e1088.

Guo, L.C., Zhang, Y., Lin, H., Zeng, W., Liu, T., Xiao, J., Rutherford, S., You, J., Ma, W., 2016. The washout effects of rainfall on atmospheric particulate pollution in two Chinese cities. Environmental Pollution 215, 195-202.

Hernández-Fernández, J., Puello-Polo, E., Trillera, J., 2022. Characterization of microplastics in total atmospheric deposition sampling from areas surrounding industrial complexes in northwestern Colombia. Sustainability 14, 13613.

Huang, Y., He, T., Yan, M., Yang, L., Gong, H., Wang, W., Qing, X., Wang, J., 2021. Atmospheric transport and deposition of microplastics in a subtropical urban environment. Journal of Hazardous Materials 416, 126168.

Jia, Q., Duan, Y., Han, X., Sun, X., Munyaneza, J., Ma, J., Xiu, G., 2022. Atmospheric deposition of microplastics in the megalopolis (Shanghai) during rainy season: Characteristics, influence factors, and source. Science of the Total Environment 847, 157609.

Klein, M., Fischer, E.K., 2019. Microplastic abundance in atmospheric deposition within the Metropolitan area of Hamburg, Germany. Science of the Total Environment 685, 96–103.

Knobloch, E., Ruffell, H., Aves, A., Pantos, O., Gaw, S., Revell, L.E., 2021. Comparison of deposition sampling methods to collect airborne microplastics in Christchurch, New Zealand. Water Air and Soil Pollution 232, 133.

Li, J., Zhang, J., Ren, S., Huang, D., Liu, F., Li, Z., Zhang, H., Zhao, M., Cao, Y., Mofolo, S., Liang, J., Xu, W., Jones, D.L., Chadwick, D.R., Liu, X., Wang, K., 2023. Atmospheric deposition of microplastics in a rural region of North China Plain. Science of the Total Environment 877, 162947.

Liu, Z., Bai, Y., Ma, T., Liu, X., Wei, H., Meng, H., Fu, Y., Ma, Z., Zhang, L., Zhao, J., 2022. Distribution and possible sources of atmospheric microplastic deposition in a valley basin city (Lanzhou, China). Ecotoxicology and Environmental Safety 233, 113353.

Perera, K., Ziajahromi, S., Nash, S.B., Manage, P.M., Leusch, F.D.L., 2022. Airborne microplastics in indoor and outdoor environments of a developing country in South Asia: Abundance, distribution, morphology, and possible sources. Environmental Science & Technology 56, 16676-16685.

Purwiyanto, A.I.S., Prartono, T., Riani, E., Naulita, Y., Cordova, M.R., Koropitan, A.F., 2022. The deposition of atmospheric microplastics in Jakarta-Indonesia: The coastal urban area. Marine Pollution Bulletin 174, 113195.

Rezaei, M., Abbasi, S., Pourmahmood, H., Oleszczuk, P., Ritsema, C., Turner, A., 2022. Microplastics in agricultural soils from a semi-arid region and their transport by wind erosion. Environmental Research 212, 113213.

Shruti, V.C., Kutralam-Muniasamy, G., Peréz-Guevara, F., Roy, P.D., Martínez, I.E., 2022. Occurrence and characteristics of atmospheric microplastics in Mexico City. Science of the Total Environment 847, 157601.

Sun, J., Peng, Z., Zhu, Z.R., Fu, W., Dai, X., Ni, B.J., 2022. The atmospheric microplastics deposition contributes to microplastic pollution in urban waters. Water Research 225, 119116.

Szewc, K., Graca, B., Dołega, A., 2021. Atmospheric deposition of microplastics in the coastal zone: Characteristics and relationship with meteorological factors. Science of the Total Environment 761, 143272.

Villanova-Solano, C., Hernández-Sánchez, C., Díaz-Peña, F.J., González-Sálamo, J., González-Pleiter, M., Hernández-Borges, J., 2023. Microplastics in snow of a high mountain national park: El Teide, Tenerife (Canary Islands, Spain). Science of the Total Environment 873, 162276.

Wright, S.L., Ulke, J., Font, A., Chan, K.L.A., Kelly, F.J.,2020. Atmospheric microplastic deposition in an urban environment and an evaluation of transport. Environ. Int. 136, 105411.

Yuan, Z., Pei, C.L., Li, H.X., Lin, L., Liu, S., Hou, R., Liao, R., Xu, X.R., 2023. Atmospheric microplastics at a southern China metropolis: Occurrence, deposition flux, exposure risk and washout effect of rainfall. Science of the Total Environment 869, 161839.

Zhang, Y., Kang, S., Allen, S., Allen, D., Gao, T., Sillanpää, M., 2020. Atmospheric microplastics: a review on current status and perspectives. Earth Science Reviews 203, 103118.